Probing the nature of the Ce 4*f* states in CeX_9Si_4 (X=Ni,Co) by high-energy electron spectroscopies

X. Wang,[1] H. Michor,[2] and M. Grioni[1]
[1]*IPN, Ecole Polytechnique Fédéderale (EPFL), CH-1015 Lausanne, Switzerland*
[2]*Institut für Festkörperphysik, TU Wien, Wiedner Hauptstrasse 8-10, A-1040 Wien, Austria*
(Received 18 October 2006; published 29 January 2007)

We have used x-ray photoelectron spectroscopy, and resonant inverse photoemission at the CeM_5($3d_{5/2}$ $\rightarrow 4f$) edge, to study the Ce 4*f* states in the isostructural metallic compounds $CeCo_9Si_4$ and $CeNi_9Si_4$. The spectroscopic data reveal the intermediate-valence nature of these materials. They also suggest that a larger density of states at the Fermi level, and a reduced 4*f* energy, are the origin of an enhanced 4*f*–conduction band hybridization in the Co compound. This provides an explanation for the remarkable differences in the magnetic, transport, and thermodynamic properties of the two materials.

DOI: 10.1103/PhysRevB.75.035127 PACS number(s): 71.28.+d, 78.70.En, 78.70.Dm, 79.60.−i

I. INTRODUCTION

Metallic Ce compounds are of great interest for the intriguing physical properties associated with the 4*f* electrons. Due to the competition of Coulomb interaction and hybridization with the conduction band, these states are intermediate between local spin and extended band states.[1] The 4*f* occupation number n_f is neither integer nor constant, and the local magnetic moments observed at high temperature are screened and compensated at sufficiently low temperature. The strongly correlated, partially localized 4*f* states yield anomalous contributions to most physical properties, including the magnetic susceptibility, the electronic specific heat, and the thermal and electrical resistivities. The main features of this intermediate-valence (IV) or "Kondo" behavior are often well described in terms of isolated Ce impurities in a metallic matrix. In the simple Anderson impurity model (AIM), but also in more general Anderson lattice models (ALMs), the anomalous quantities exhibit an approximate scaling as a function of the single parameter (T/T_K). The material-dependent Kondo temperature T_K represents the energy gained in the formation of the nonmagnetic ground state, and grows exponentially with the 4*f*-band hybridization strength.[2,3]

In this paper we analyze the Ce valence and hybridization strength of two isostructural cerium Kondo-lattice compounds $CeNi_9Si_4$ and $CeCo_9Si_4$ with almost equal unit cell volumes ($\Delta V/V=5.56\times10^{-3}$) but remarkably different degrees of hybridization. $CeNi_9Si_4$ is an archetypal Kondo-lattice system. It exhibits thermodynamic properties that are very well described by the integer-valent limit of the AIM, the Coqblin-Schrieffer model, for a fully degenerate Ce^{3+} ($J=5/2$) ion, with a characteristic temperature $T_0\simeq180$ K. The Wilson ratio $R\simeq1.25$ is also in close agreement with the theoretical value for a six-fold degenerate Ce^{3+} state.[4] Remarkable agreement with ALM results by Cox and Grewe[5] was also observed for transport properties. In particular, the analysis of the thermoelectric power yields a Kondo temperature $T_K\sim80$ K in agreement with the above T_0, according to the theoretical ratio $T_K/T_0\simeq0.43$ for $J=5/2$ by Schlottmann.[6]

Replacing Ni by Co in the isostructural compound $CeCo_9Si_4$ leads to remarkably different physics originating from the different features of the Ni and Co 3*d* bands, and to more strongly hybridized 4*f* states.[7] The isostructural reference systems $LaNi_9Si_4$ and $LaCo_9Si_4$ reveal for the Ni 3*d* bands simple Pauli paramagnetic behavior with moderate Stoner-enhancement $S\leq2$ but strongly correlated nearly magnetic Co 3*d* bands with large Stoner enhancement $S\sim20$ and itinerant electron metamagnetism at rather low fields of about 3–6 T.[4,8] While it proved to be straightforward to extract the 4*f* Kondo contribution to the specific heat and magnetic susceptibility of $CeNi_9Si_4$ by subtracting the $LaNi_9Si_4$ reference data as background, it would clearly be misleading to use $LaCo_9Si_4$ as a background reference for $CeCo_9Si_4$. Both the low-temperature electronic specific heat coefficient $\gamma\simeq190$ mJ/mol K^2 and the magnetic susceptibility $\chi_0\simeq30\times10^{-3}$ emu/mol (Refs. 7 and 9) are in fact smaller than $\gamma\simeq200$ mJ/mol K^2 and $\chi_0\simeq51\times10^{-3}$ emu/mol of $LaCo_9Si_4$ (see Refs. 4, 7, and 8). Simply using γ and χ_0 to estimate T_K and the degree of hybridization of the 4*f* states in $CeCo_9Si_4$ is questionable, and yields values that are inconsistent with structural data. The latter suggest a rather strong hybridization, since the reduction of the unit cell volume of $CeCo_9Si_4$ as compared to $LaCo_9Si_4$, $\Delta V/V=-12.0\times10^{-3}$, is significantly larger than is the case of $CeNi_9Si_4$ and $LaNi_9Si_4$, $\Delta V/V=-9.1\times10^{-3}$. It is also much larger than $\Delta V/V\sim-7\times10^{-3}$, the value expected from the trend due to the lanthanide contraction in $R^{3+}Co_9Si_4$, with R^{3+}=La, Pr, Nd,…, for hypothetical $Ce^{3+}Co_9Si_4$.

High-energy electron spectroscopies, namely photoemission (PES) and inverse photoemission (IPES), provide a view of the Ce electronic configuration that is complementary to low-energy magnetic, transport, or thermodynamic probes.[10,11] The PES and IPES spectra directly probe the 4*f* spectral function, namely, the characteristic many-body Kondo resonance (KR). They also yield quantitative information on configuration mixing in the IV ground state, and on the density of states (DOS) at the Fermi level, which plays a key role in determining the 4*f*-band hybridization strength. Comparing the PES and IPES spectral response of $CeCo_9Si_4$ and $CeNi_9Si_4$ can therefore reveal and clarify differences in the nature of the 4*f* states in the two compounds. Here we report core level and valence band PES as well as resonant IPES (RIPES) measurements. Both compounds ex-

hibit the spectroscopic signatures of IV materials. A comparison of the valence band PES spectra reveals a higher density of conduction states at the Fermi level and a lower $4f$ binding energy in $CeCo_9Si_4$. Within a Kondo scenario, these differences are the likely origin of the stronger $4f$-band hybridization in $CeCo_9Si_4$, and ultimately of the differences in the electronic properties of the two materials.

II. EXPERIMENT

Polycrystalline $CeCo_9Si_4$ was prepared by high-frequency induction melting under protective Ar (99.9999%) atmosphere. The starting materials are cerium ingots (99.98% purity, Ames Materials Preparation Center, USA), cobalt ingots (99.995%, Alpha Aesar, Ward Hill, MA, USA), and silicon pieces (99.9999%, Alpha Aesar) melted together in a two-step procedure. Initially, Co and Si were melted together and remelted four times. In a second step Ce was melted together with the precursor Co_9Si_4 alloy. To ensure homogeneity and phase purity, the buttons were broken, flipped over, and remelted another five times and finally sealed in an evacuated quartz tube and annealed at 1050 °C for 10 days. The polycrystalline $CeNi_9Si_4$ material used in the present investigation is identical with that characterized earlier in Ref. 4.

We performed PES and RIPES measurements at Lausanne. The specimens were mounted on a flow cryostat, and clean surfaces were prepared in vacuum by repeatedly scraping with a diamond file, at a base pressure in the low 10^{-10} mbar range. For the PES measurements we used a Scienta ESCA300 spectrometer, equipped with a monochromatized Al $K\alpha(h\nu=1486$ eV) source, and a hemispherical electrostatic analyzer. The overall energy resolution was $\Delta E=0.4$ eV. The RIPES spectrometer is based on a slitless crystal spectrograph in a dispersive Bragg geometry, described in Ref. 12. For measurements at the CeM_5 edge ($\sim$881 eV) we used a beryl $(10\bar{1}0)$ crystal, with an overall resolution of $\sim$1 eV.

III. RESULTS AND DISCUSSION

Figure 1 illustrates the Ce $3d$ core level PES spectra of $CeNi_9Si_4$, $CeCo_9Si_4$, and of selected reference Ce materials, from the literature.[13,14] The Ce $3d$ PES line shape of IV Ce systems is complex. First of all, the spectrum is split by the large ($\sim$20 eV) $3d$ spin-orbit interaction into two partially overlapping $j=5/2$ and $j=3/2$ manifolds. Each spin-orbit partner is further split into three features corresponding to PES final states with (mainly) 0, one, or two $4f$ electrons. The order of the $4f$ configurations in the final state (f^2, f^1, and f^0) is different from that of the neutral initial state (f^1, f^0, and f^2)as a result of the large attractive Coulomb interaction ($\sim$8 eV per $4f$ electron) with the $3d$ core hole. The relative intensities of the PES features are determined by their coupling with the mixed ground state. The f^0 peak, in particular, corresponds to an almost pure f^0 final state, and its intensity is an excellent indicator of the quantity $(1-n_f)$ in the ground state, and therefore of the Ce valence $v=3+(1-n_f)$.[13,15] It is very small in materials like, e.g., Ce_7Ni_3 [Fig. 1(a)], where the $4f$-band hybridization is small, and large in strongly hybridized materials like $CeRh_3$ [Fig. 1(d)].

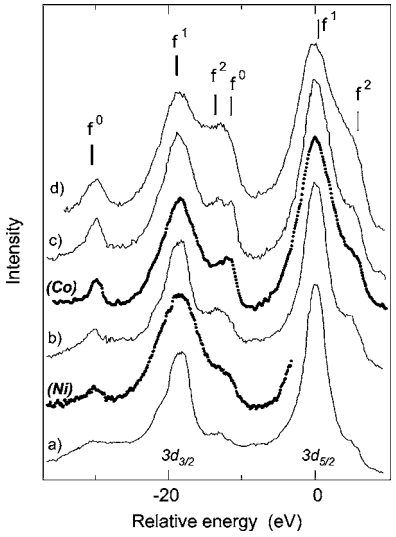

FIG. 1. PES spectra of the Ce $3d$ core levels of $CeNi_9Si_4$, $CeCo_9Si_4$, and of selected IV Ce compounds. (a) Ce_7Ni_3, (Ni), $CeNi_9Si_4$; (b) CeNi; (Co), $CeCo_9Si_4$; (c) $CeNi_2$; (d) $CeRh_3$. Vertical ticks mark the various final states (thick $3d_{3/2}$; thin $3d_{5/2}$).

These qualitative considerations can be put on a quantitative basis within the framework of the AIM,[16] and a very satisfactory agreement with experiment has been achieved by adopting configuration-dependent parameters.[17,18] Determining the absolute n_f values from PES requires a rather elaborate analysis to separate contributions from the (less hybridized) surface Ce ions. Figure 1 illustrates a more qualitative approach, based on a comparison with reference compounds, spanning a wide range of hybridization strengths. The energy reference is set at the peak position of the $j=5/2$ (f^1) feature (the actual binding energy is $E_B=881$ eV), and the spectrum of $CeNi_9Si_4$ is truncated on the high-energy side, where it overlaps with a very strong Ni $2p$ core feature. The larger intensity of the (f^0) feature indicates an increasing configuration mixing from $CeNi_9Si_4$ to $CeCo_9Si_4$. The spectrum of $CeNi_9Si_4$ is intermediate between those of Ce_7Ni_3—an antiferromagnet, with $T_K\sim 2$ K,[19] $n_f\sim 1$—and of CeNi, with estimated $T_K\sim 100-140$ K and $n_f>0.9$.[20,21] The spectrum of $CeCo_9Si_4$ is similar to that of $CeNi_2$, a compound that is near the limit of validity of the AIM, with estimated $T_K>1000$ K (Ref. 22) and $n_f\sim 0.83$.[10] The $3d$ core level results show that $CeNi_9Si_4$ to $CeCo_9Si_4$ are IV compounds, and indicate a strong enhancement of the $4f$-band hybridization in the latter, consistent with a much higher T_K.

The origin of the larger hybridization in $CeCo_9Si_4$ is clarified by the PES valence band (VB) spectra, shown in Fig. 2 after the usual subtraction of an inelastic Shirley background. They reflect the momentum-integrated density of states, and are dominated by the Ni and Co $3d$ bands at and just below the Fermi level E_F. Additional structures in the 4–7 eV range can be assigned to Si sp hybrid states. A shoulder at $\sim$2.3 eV in $CeNi_9Si_4$ is the signature of the Ce $4f$ states. It corresponds to the "ionization" (f^0) final state. This signal is weak due to the low Ce concentration, and also to the unfa-

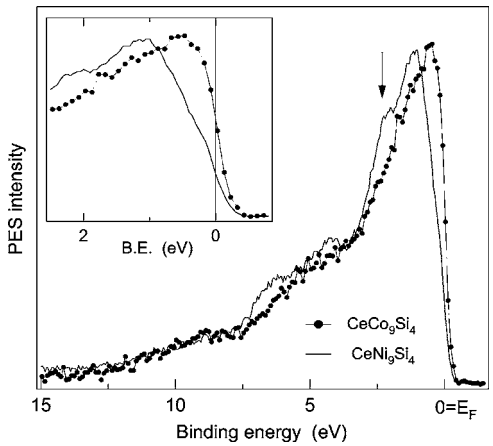

FIG. 2. Valence band PES spectra of $CeNi_9Si_4$ and $CeCo_9Si_4$ measured at 300 K ($h\nu$=1486 eV). The arrow marks the "ionization" (f^0) final state in $CeNi_9Si_4$. The inset shows a closeup of the spectra near the Fermi level.

vorable cross section at this large photon energy.[23] The absence of a similar discernible feature in the Co compound is consistent with the expected transfer of spectral weight from the ionization peak to the KR feature above E_F as the hybridization increases. The main difference between the data is a ~0.5 eV rigid shift toward higher binding energy of the $CeNi_9Si_4$ line shape, reflecting the addition of one extra 3*d* electron in the Ni 3*d* band. In the inset of Fig. 2 the peak of the Co 3*d* band at $E\sim0.5$ eV is barely distinguishable from the onset of the metallic Fermi edge. By contrast, the maximum of the Ni 3*d* band at 1 eV is well separated from the metallic Fermi step at E_F. The data show that the 3*d* DOS at E_F is larger in $CeCo_9Si_4$ than in $CeNi_9Si_4$ by a factor of 2. We notice that specific heat data and band structure calculations indicate a similar increase in the corresponding La compounds, from ~10 states/eV ($LaNi_9Si_4$) (Refs. 4 and 24) to 19 states/eV ($LaCo_9Si_4$).[8]

The twofold increase of the 3*d* DOS at E_F in $CeCo_9Si_4$ has a large impact on the electronic properties. Within the AIM, $T_K \approx D\exp(-\pi\varepsilon_f/N\Gamma)$, where D is the bandwidth, ε_f is the bare 4*f* binding energy, and N is the degeneracy of the 4*f* states.[2] The "hybridization width" $\Gamma=\pi\rho(E_F)V^2$ is proportional to the conduction band DOS at E_F, $\rho(E_F)$, and to the square of a 4*f*-band hopping matrix element. The parameters D, N, and V should have similar values in the two isostructural compounds. On the other hand, in a rigid band scenario, the bare energy of the 4*f*states is probably tied to the centroid of the conduction band, and ε_f is therefore reduced from ~2.3 eV in $CeCo_9Si_4$, to ~1.8 eV in $CeNi_9Si_4$. These simple considerations suggest that T_K should increase by a factor ~4–5 between $CeNi_9Si_4$ and $CeCo_9Si_4$ as a result of the combined changes in $\rho(E_F)$ and ε_f.

In Ce-based materials the valence band PES spectrum contains only the occupied tail of the many-body KR, whose maximum is located above E_F. This signal is too weak to be distinguished from the strong 3*d* band in Fig. 2. The KR can be probed by IPES, which is sensitive to the electron-addition, "unoccupied" part of the many-body spectral function $A(\omega)$.[11] Since the Ce concentration is low in our compounds, the measured KR intensity is also weak, but the Ce 4*f* spectral function can be strongly enhanced by an appropriate choice of the excitation energy. In a resonant IPES experiment, the energy E_{in} of the exciting electron beam is chosen to coincide with the binding energy of a Ce 3*d* or 4*d* core level.[25–27] As for the more common resonant PES, the resonant enhancement in RIPES is due to the interference of two transition channels sharing the same initial and final states. In RIPES the normal IPES channel $4f^N+e\rightarrow4f^{N+1}+h\nu$ interferes with the indirect channel $4f^N+e\rightarrow3d^94f^{N+2}\rightarrow4f^{N+1}+h\nu$. Due to the localized nature of the 3*d* core hole, and to dipole selection rules, RIPES mainly reflects the 4*f* part of the addition spectrum, projected on the Ce site. RIPES is a second-order coherent process, and specific aspects of the spectral weight distribution depend not only on the ground state, but also on the intermediate state, which contains a core hole. Detailed calculations can be performed in the framework of the AIM,[28] but a direct comparison of the spectra already gives important indications on the nature of the 4*f* electrons.

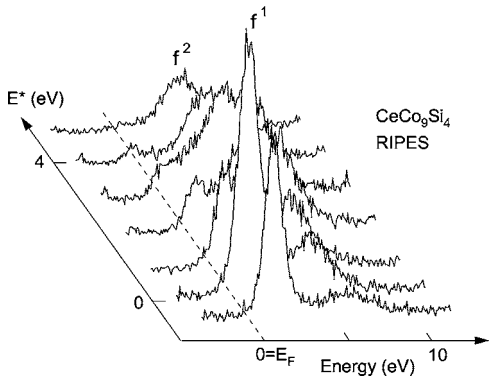

FIG. 3. RIPES of $CeCo_9Si_4$ near the Ce$3d_{5/2}$ (M_5) threshold. Spectra measured at increasing incident energy $E_{in}=E^*+881$ eV have been vertically offset for clarity.

Figure 3 shows typical RIPES results for $CeCo_9Si_4$. Each curve represents the energy distribution of the emitted photons, for a fixed incident electron energy E_{in}. The horizontal axis measures, as in conventional IPES, the final state excitation energy $E=[h\nu_{out}(\max)-h\nu_{out}]$, and the high emitted photon energy limit $h\nu_{out}(\max)$ coincides with E_F. Different spectra correspond to different incident energies ($E_{in}=881$ eV$+E^*$) around the Ce$3d_{5/2}$(M_5) threshold, and the curves have been vertically offset for clarity. The (f^1) final state feature (the KR) exhibits a sharp maximum at $E^*=0$, while the intensity of the broader (f^2) multiplet has a delayed maximum at $E^*\sim2-3$ eV, in agreement with RIPES data on other Ce IV materials.[26]

The large spectral changes that occur as a function of the incident energy in the resonance region are clearly illustrated in Fig. 4(a), which compares the $E^*=0$ and $E^*=3$ eV spectra of $CeNi_9Si_4$. At $E^*=0$ the KR near E_F dominates the IPES line shape, but its intensity decreases by roughly one order of magnitude at $E^*=3$, where the broad (f^2) multiplet is in its turn enhanced. Relative changes in the KR intensity as a function of external parameters like temperature or stoichiometry are therefore best studied at $E^*=0$. Figure 4(b) shows

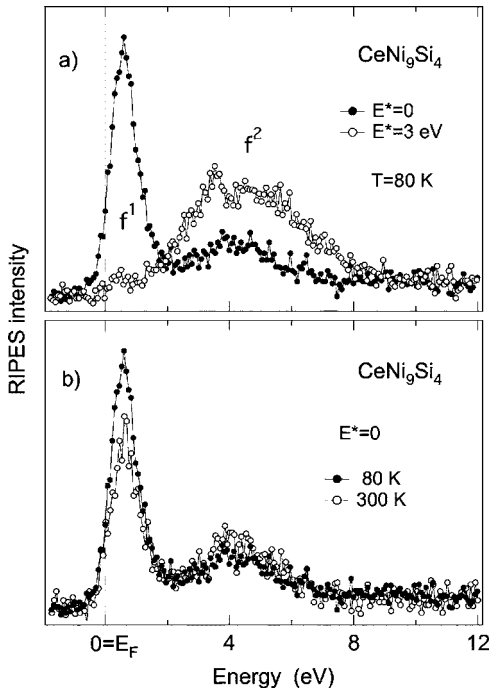

FIG. 4. (a): RIPES spectra of $CeNi_9Si_4$ measured at 80 K at the maxima of the f^1 ($E^*=0$) and f^2 ($E^*=3$ eV) resonances. (b) Comparison of the $E^*=0$ spectra at 80 and 300 K.

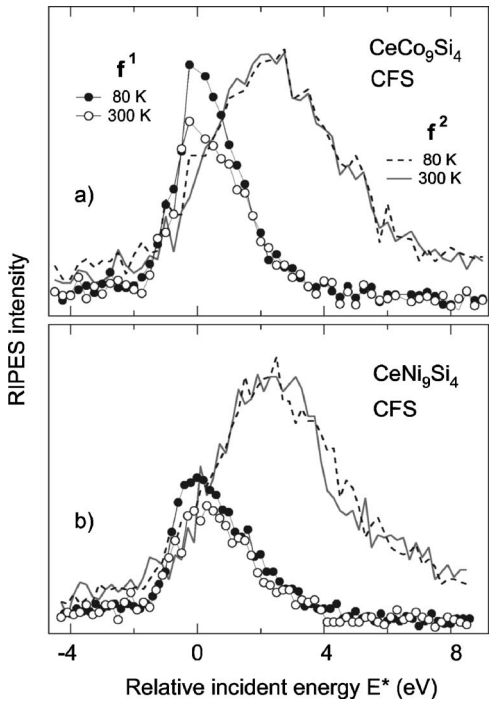

FIG. 5. Constant final state (CFS) curves of (a) $CeCo_9Si_4$ and (b) $CeNi_9Si_4$ showing the separate f^1 and f^2 resonance profiles. CFS curves measured at 80 and 300 K have been arbitrarily normalized to the maximum of the f^2 resonance.

the temperature evolution between 80 and 300 K under these conditions. The intensity of the KR decreases at the higher temperature, as low-lying magnetic (f^1) excited states become thermally populated.[2,11] It should be noticed that the intensity lost by the KR is only partly compensated by an increase of the f^2 intensity: the total spectral weight is not conserved at resonance, since the intensity enhancement is different for different final states. Therefore the simple f^1/f^2 intensity ratio does not entirely determine the initial state Ce configuration.

The Ce valence state can still be estimated from a comparison of the separate f^1 and f^2 resonance intensity profiles, as discussed in Ref. 26. The constant final state (CFS) curves of Fig. 5 represent the integrated f^1 and f^2 IPES intensities, measured within two separate energy windows, while varying the incident energy across the Ce M_5 threshold. They illustrate the sharp enhancement of the f^1 emission at E^*, and the broader f^2 maximum around $E^*=2-3$ eV. For each compound, CFS curves collected at 300 and 80 K are shown, arbitrarily normalized to the same f^2 peak intensity. The ratio R of the maxima of the f^1 and f^2 CFS profiles in different Ce-based IV materials grows with the weight of the f^0 configuration in the initial state. From Fig. 5 we find $R\sim 1$ for $CeCo_9Si_4$ at 80 K, which is somewhat smaller than the corresponding values for strongly hybridized systems like $CeFe_2$ ($R=1.2$) and $CeNi_2$ ($R=1.37$).[26] The smaller $R\sim 0.56$ for $CeNi_9Si_4$ at 80 K is typical for moderately hybridized Kondo systems like, e.g., $CePd_3$ ($T_K\sim 240$ K).[26] This is consistent with the conclusions drawn from the PES data of Fig. 1. The results of Fig. 5 also show that R decreases from 80 to 300 K, as already suggested by the data of Fig. 4, in agreement with the characteristic Kondo temperature dependence of n_f. It is interesting that the temperature change is visible for both compounds despite the considerably different T_K values. According to the AIM the temperature-driven change Δn_f occurs almost entirely between $T\sim(T_K/3)$ and $T\sim 3T_K$.[2] For $CeNi_9Si_4$ ($T_K\sim 80$ K) the measurement covers a substantial part of the temperature range of interest, from T_K to $\sim 4T_K$. On the other hand, the observation of a clear temperature dependence sets a rough upper limit $T_K<(2-3)\times 300$ K for $CeCo_9Si_4$. This, again, is compatible with the T_K enhancement between $CeNi_9Si_4$ and $CeCo_9Si_4$ expected from the VB PES data of Fig. 2.

IV. SUMMARY

We have studied by core level and valence band x-ray photoelectron spectroscopy, and by resonant inverse photoemission, the electronic configuration of the two isostructural Ce compounds $CeNi_9Si_4$ and $CeCo_9Si_4$. A comparison with other typical Ce-based IV materials shows that $CeNi_9Si_4$ is a moderately hybridized Kondo system. The $4f$-band hybridization is larger in $CeCo_9Si_4$ as a result of a larger d density of states at the Fermi level, and of the reduced $4f$ binding energy. For $\rho(E_F)$ we observe the same twofold increase previously determined for the corresponding La compounds. From AIM relations we estimate a corresponding increase of the characteristic Kondo temperature T_K by a factor $\sim 4-5$ which explains, at least qualitatively, the remarkable differences of the $4f$-related properties in the two compounds. This value should be considered as a lower limit for the ratio of the two T_K's. In fact, the $4f$-band hybridization is often

reduced in the near-surface region probed by electron spectroscopies, and the effect is proportionally larger in large T_K materials.[29,30] A complementary investigation by photon-in–photon-out spectroscopies like high-resolution x-ray absorption or resonant inelastic x-ray scattering,[31,32] which are less sensitive to the surface layer, could yield a more accurate quantitative estimation of the bulk T_K's. Nevertheless, we anticipate that such quantitative refinement will not influence the main qualitative results of the present study, which confirms the interest of combining traditional "low-energy" and "high energy" spectroscopic data for a deeper understanding of IV materials.

ACKNOWLEDGMENTS

We gratefully acknowledge very useful correspondence with D. Malterre and N. Witkowski. The work in Lausanne is supported by the Swiss National Science Foundation and by the NCCR MaNEP.

[1] P. A. Lee, T. M. Rice, J. W. Serene, L. S. Sham, and J. W. Wilkins, Comments Condens. Matter Phys. **12**, 99 (1986).
[2] N. E. Bickers, D. L. Cox, and J. W. Wilkins, Phys. Rev. B **36**, 2036 (1987).
[3] A. C. Hewson, *The Kondo Problem to Heavy Fermions* (Cambridge University Press, Cambridge, U.K., 1993).
[4] H. Michor, St. Berger, M. El-Hagary, C. Paul, E. Bauer, G. Hilscher, P. Rogl, and G. Giester, Phys. Rev. B **67**, 224428 (2003).
[5] D. L. Cox and N. Grewe, Z. Phys. B: Condens. Matter **71**, 321 (1988).
[6] P. Schlottmann, Z. Phys. B: Condens. Matter **51**, 223 (1983).
[7] M. El-Hagary, H. Michor, E. Bauer, R. Grössinger, P. Kerschl, D. Eckert, K.-H. Müller, P. Rogl, G. Giester, and G. Hilscher, Physica B **359-361**, 311 (2005).
[8] H. Michor, M. El-Hagary, M. D. Mea, M. W. Pieper, M. Reissner, G. Hilscher, S. Khmelevskyi, P. Mohn, G. Schneider, G. Giester, and P. Rogl, Phys. Rev. B **69**, 081404(R) (2004).
[9] More recent results yield $\chi_0 \sim 17 \times 10^{-3}$ emu/mol. The discrepancy is due to a ferromagnetic impurity phase in the sample used in Ref. 7; H. Michor and M. Giovannini (unpublished).
[10] J. W. Allen, S.-J. Oh, O. Gunnarsson, K. Schönhammer, M. B. Maple, M. S. Torikachvili, and I. Lindau, Adv. Phys. **35**, 275 (1986).
[11] D. Malterre, M. Grioni, and Y. Baer, Adv. Phys. **45**, 299 (1986).
[12] P. Weibel, M. Grioni, C. Heche, and Y. Baer, Rev. Sci. Instrum. **66**, 3755 (1995).
[13] J. C. Fuggle, F. U. Hillebrecht, Z. Zolnierek, R. Lässer, Ch. Freiburg, O. Gunnarsson, and K. Schönhammer, Phys. Rev. B **27**, 7330 (1983).
[14] L. Duó, P. Vavassori, L. Braicovich, N. Witkowski, D. Malterre, M. Grioni, Y. Baer, and G. Olcese, Z. Phys. B: Condens. Matter **103**, 63 (1997).
[15] J. Krill, J.-P. Kappler, A. Meyer, L. Abadli, and M. F. Ravet, J. Phys. F: Met. Phys. **11**, 1713 (1981).
[16] O. Gunnarsson and K. Schönhammer, Phys. Rev. B **28**, 4315 (1983).
[17] O. Gunnarsson and O. Jepsen, Phys. Rev. B **38**, 3568 (1988).
[18] N. Witkowski, F. Bertran, and D. Malterre, Phys. Rev. B **56**, 15040 (1997).
[19] K. Umeo, H. Kadomatsu, and T. Takabatake, Phys. Rev. B **54**, 1194 (1996).
[20] D. Gignoux, F. Givord, and R. Lemaire, J. Less-Common Met. **94**, 165 (1983).
[21] J. I. Espeso, J. C. Gomez Sal, and J. Chaboy, Phys. Rev. B **63**, 014416 (2000).
[22] A. P. Murani and R. S. Eccleston, Phys. Rev. B **53**, 48 (1997).
[23] J. J. Yeh and I. Lindau, At. Data Nucl. Data Tables **32**, 1 (1985).
[24] S. Khmelevskyi (private communication).
[25] P. Weibel, M. Grioni, D. Malterre, B. Dardel, and Y. Baer, Phys. Rev. Lett. **72**, 1252 (1994).
[26] M. Grioni, P. Weibel, D. Malterre, Y. Baer, and L. Duó, Phys. Rev. B **55**, 2056 (1997).
[27] K. Kanai, T. Terashima, A. Kotani, T. Uozumi, G. Schmerber, J. P. Kappler, J. C. Parlebas, and S. Shin, Phys. Rev. B **63**, 033106 (2001).
[28] A. Tanaka and T. Jo, J. Phys. Soc. Jpn. **65**, 615 (1996).
[29] E. Weschke, C. Laubschat, T. Simmons, M. Domke, O. Strebel, and G. Kaindl, Phys. Rev. B **44**, 8304 (1991).
[30] A. Sekiyama, T. Iwasaki, K. Matsuda, Y. Saitoh, Y. Onuki, and S. Suga, Nature (London) **403**, 396 (2000).
[31] C. Dallera, M. Grioni, A. Shukla, G. Vanko, J. L. Sarrao, J. P. Rueff, and D. L. Cox, Phys. Rev. Lett. **88**, 196403 (2002).
[32] A. Kotani, Eur. Phys. J. B **47**, 3 (2005).